resulting in substantially increased hydraulic gradients on the coastal plain. The more distant outlets of the groundwater flow, combined with greater hydraulic gradients, likely resulted in much deeper circulation of fresh water than at present. When sea level rose during the Pleistocene-Holocene transition, hydraulic gradients greatly decreased, and the Pleistocene groundwater in the lower parts of the aquifer was disconnected from the active flow system above. The reduced hydraulic gradients and resulting shallower groundwater circulation also prevented flushing of this part of the aquifer during the subsequent early to mid Holocene wet period.

References and Notes

1. E. Bard, *Science* **284**, 1133 (1999).
2. J. E. Kutzbach and P. J. Guetter, *J. Atmos. Sci.* **43**, 1726 (1986); A. J. Broccoli and S. Manabe, *Clim. Dyn.* **1**, 87 (1987).
3. R. S. Webb, D. H. Rind, S. J. Lehman, R. J. Healy, D. Sigman, *Nature* **385**, 695 (1997); S. W. Hostetler and A. C. Mix, *Nature* **399**, 673 (1999).
4. A. B. G. Bush and S. G. H. Philander, *Science* **279**, 1341 (1998); A. Ganopolski, S. Rahmstorf, V. Petoukhov, M. Claussen, *Nature* **391**, 351 (1998).
5. CLIMAP: Climate/Long-Range Investigation, Mapping and Prediction Project Members, *Geol. Soc. Am. Map Chart Ser. 36* (1981); *Science* **191**, 1131 (1976).
6. R. Thunell, D. Anderson, D. Gellar, Q. Miao, *Quat. Res.* **41**, 255 (1994); L. D. Stott and C. M. Tang, *Paleoceanography* **11**, 37 (1996).
7. W. Broecker, *Quat. Res.* **26**, 121 (1986).
8. J. C. Duplessy, *Nature* **295**, 494 (1982); W. L. Prell *et al.*, *Quat. Res.* **14**, 309 (1980).
9. E. L. Sikes and L. D. Keigwin, *Paleoceanography* **9**, 31 (1994); A. C. Mix, W. F. Ruddiman, A. McIntyre, *Paleoceanography* **1**, 43 (1986); A. C. Mix, W. F. Ruddiman, A. McIntyre, *Paleoceanography* **1**, 339 (1986); R. Schneider, P. J. Mueller, G. Ruhland, *Paleoceanography* **10**, 197 (1995).
10. E. Bard, F. Rostek, C. Sonzogni, *Nature* **385**, 707 (1997); F. Rostek *et al.*, *Nature* **364**, 319 (1993).
11. The $\delta^{18}O$ notation is
$$\delta^{18}O = \left[\frac{(^{18}O/^{16}O)_{sample}}{(^{18}O/^{16}O)_{std}} - 1 \right] \times 1000$$
where std is the standard mean ocean water reference.
12. T. P. Guilderson, R. G. Fairbanks, J. L. Rubenstone, *Science* **263**, 663 (1994); J. W. Beck *et al.*, *Science* **257**, 644 (1992); J. W. Beck, J. Récy, F. Taylor, R. L. Edwards, G. Cabioch, *Nature* **385**, 705 (1997).
13. C. M. Clapperton, *Palaeogeogr. Palaeoclimatol. Palaeoecol.* **101**, 189 (1993).
14. P. Webster and N. Streten, *Quat. Res.* **10**, 279 (1978); D. Rind and D. Peteet, *Quat. Res.* **24**, 1 (1985).
15. M. B. Bush, P. A. Colinvaux, M. C. Wieman, D. R. Piperno, K. b. Liu, *Quat. Res.* **34**, 330 (1990); M. B. Bush *et al.*, *Ecol. Monogr.* **62**, 251 (1992).
16. B. W. Leyden, M. Brenner, D. A. Hodell, J. H. Curties, in *Climate Change in Continental Isotopic Records*, vol. 78 of *Geophysical Monograph Series*, P. K. Swart, K. C. Lohmann, J. McKenzie, S. Savin, Eds. (American Geophysical Union, Washington, DC, 1993), pp. 156–178; K. b. Liu and P. A. Colinvaux, *Nature* **318**, 556 (1985).
17. L. G. Thompson *et al.*, *Science* **269**, 46 (1995); L. G. Thompson *et al.*, *Science* **282**, 1858 (1998).
18. R. T. Pierrehumbert, *Geophys. Res. Lett.* **26**, 1345 (1999).
19. M. Stute *et al.*, *Science* **269**, 379 (1995).
20. M. Stute and A. S. Talma, in *Isotope Techniques in the Study of Environmental Change* (International Atomic Energy Agency, Vienna, 1998), pp. 307–318; W. M. Edmunds, E. Fellman, I. B. Goni, G. McNeill, D. D. Harkness, in *Isotope Techniques in the Study of Environmental Change* (International Atomic Energy Agency, Vienna, 1998), pp. 693–707; W. M. Edmunds, E. Fellman, I. B. Goni, *J. Geol. Soc. London* **156**, 345 (1999).
21. E. Mazor, *Geochim. Cosmochim. Acta* **36**, 1321 (1972); M. Stute and P. Schlosser, in *Climate Change in Continental Isotopic Records*, vol. 78 of *Geophysical Monograph Series*, P. K. Swart, K. C. Lohmann, J. McKenzie, S. Savin, Eds. (American Geophysical Union, Washington, DC, 1993), pp. 89–100.
22. The δ^2H notation is
$$\delta^2H = \left[\frac{(^2H/^1H)_{sample}}{(^2H/^1H)_{std}} - 1 \right] \times 1000$$
where std is the standard mean ocean water reference.
23. W. Dansgaard, *Tellus* **16**, 436 (1964); K. Rozanski, L. Araguás-Araguás, R. Gonfiantini, *Science* **258**, 981 (1992); in *Climate Change in Continental Isotopic Records*, vol. 78 of *Geophysical Monograph Series*, P. K. Swart, K. C. Lohmann, J. McKenzie, S. Savin, Eds. (American Geophysical Union, Washington, DC, 1993), pp. 1–36.
24. S. Hastenrath, *Climate and Circulation of the Tropics* (Reidel, Dordrecht, Netherlands, 1985).
25. D. E. Pedgely, *Weather* **24**, 456 (1969); *Meteorol. Mag.* **99**, 29 (1970).
26. C. E. Weyhenmeyer, S. J. Burns, H. N. Waber, A. Matter, unpublished data.
27. Groundwater residence times were calculated by correcting measured ^{14}C values for chemical reactions along the groundwater flow path (i.e., soil CO_2 exchange and mineral dissolution and precipitation) with the mass balance code NETPATH version 2.0 [L. N. Plummer, E. C. Prestemon, D. L. Parkhurst, *U.S. Geol. Surv. Water Resour. Invest. Rep. 94-4169* (1994)].
28. M. Stuiver *et al.*, *Radiocarbon* **40**, 1041 (1998).
29. In the inverse method to determine NGT, models describing the concentrations of atmospheric noble gases He (not used in this study), Ne, Ar, Kr, and Xe by the temperature-dependent solubility equilibrium concentrations plus a possibly fractionated excess air component are inverted to obtain the best estimates for the model parameters, including temperature [W. Aeschbach-Hertig, F. Peeters, U. Beyerle, R. Kipfer, *Water Resour. Res.* **35**, 2779 (1999)]. Recently, C. J. Ballentine and C. M. Hall [*Geochim. Cosmochim. Acta* **63**, 2315 (1999)] used the inverse approach to show that available excess air models are insufficient to describe the fractionation observed in the noble gas records from several locations, including Brazil (*19*). This described problem is overcome by a model explaining excess air fractionation by equilibration of groundwater with entrapped air (W. Aeschbach-Hertig, F. Peeters, U. Beyerle, R. Kipfer, unpublished data). This model yields good fits for nine samples from Oman. Two samples cannot be described by any currently known model, and hence no NGT could be calculated (*30*).
30. See supplementary table available at www.sciencemag.org/feature/data/1045634.shl.
31. F. Sirocko *et al.*, *Nature* **364**, 322 (1993).
32. S. C. Clemens, W. Prell, D. Murray, G. Shimmield, G. Weedon, *Nature* **353**, 720 (1991).
33. F. Sirocko, M. Sarnthein, H. Lange, H. Erlenkeuser, *Quat. Res.* **36**, 72 (1991).
34. Because of the temperature dependence of fractionation processes, the glacial-interglacial temperature increase of 6.5°C should be reflected by more negative $\delta^{18}O$ and δ^2H values in the Late Pleistocene groundwater compared with modern groundwater. In the low latitudes, however, the $\delta^{18}O$ signal appears to be more affected by the amount and source of precipitation rather than by temperature [J. R. Lawrence and S. D. Gedzelman, *Geophys. Res. Lett.* **23**, 527 (1996)].
35. E. Van Campo, *Quat. Res.* **26**, 376 (1986).
36. F. A. Street and A. T. Grove, *Quat. Res.* **12**, 83 (1979).
37. F. Gasse, R. Tehet, A. Durand, E. Gilbert, J. C. Fontes, *Nature* **346**, 141 (1990).
38. S. Burns, A. Matter, N. Frank, A. Mangini, *Geology* **26**, 499 (1998).
39. R. G. Fairbanks, *Nature* **342**, 637 (1989).

40. We thank the Ministry of Water Resources (MWR) of the Sultanate of Oman for their permission to conduct this fieldwork as well as for their logistic and scientific support; Z. Al Suleimani, former Director of Research, and P. Macumber, former Head of the Groundwater Section, MWR, for their assistance during various stages of this project; and U. Beyerle and S. Reese for their laboratory work.

22 September 1999; accepted 10 December 1999

Cross-Species Interactions Between Malaria Parasites in Humans

Marian C. Bruce,[1]* Christl A. Donnelly,[1] Michael P. Alpers,[2] Mary R. Galinski,[3] John W. Barnwell,[4] David Walliker,[5] Karen P. Day[1]

The dynamics of multiple *Plasmodium* infections in asymptomatic children living under intense malaria transmission pressure provide evidence for a density-dependent regulation that transcends species as well as genotype. This regulation, in combination with species- and genotype-specific immune responses, results in nonindependent, sequential episodes of infection with each species.

In malaria-endemic regions, humans commonly harbor chronic *Plasmodium* infections consisting of complex mixtures of different species (*1*) and genotypes of parasites (*2*). Longitudinal studies of animal malaria infections have shown that infection dynamics are affected by cross-species immunity, resulting in within-host interactions between species [reviewed in (*3*)]. Direct evidence for the action of cross-species immunity in human malaria infections has been lacking. Consecutive experimental infections with different species and genotypes indicated that immunity to human malaria is species- and genotype-specific (*4*). Data on the dynamics of simultaneous multispecies (*5*) and multigenotype coinfections (*6*) are available from only a few experiments. In some instances of mixed infections of *P. falciparum* and *P. vivax*, replacement of one species with anoth-

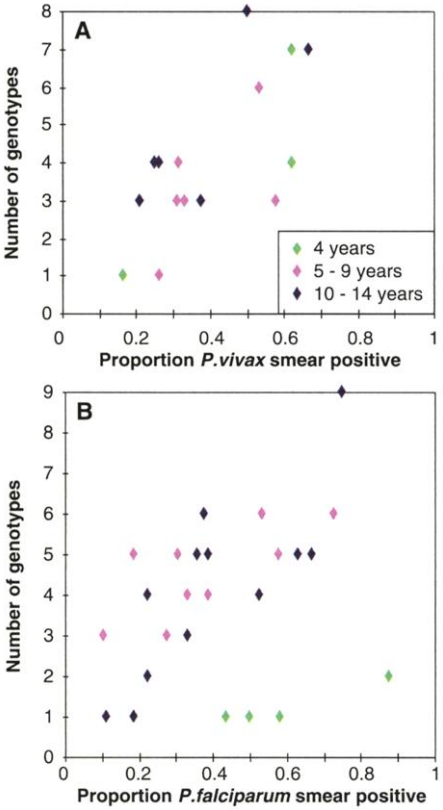

Fig. 1. Plot of number of genotypes of (**A**) *P. vivax* and (**B**) *P. falciparum* per child against the proportion of smears positive under microscopic analysis for each species.

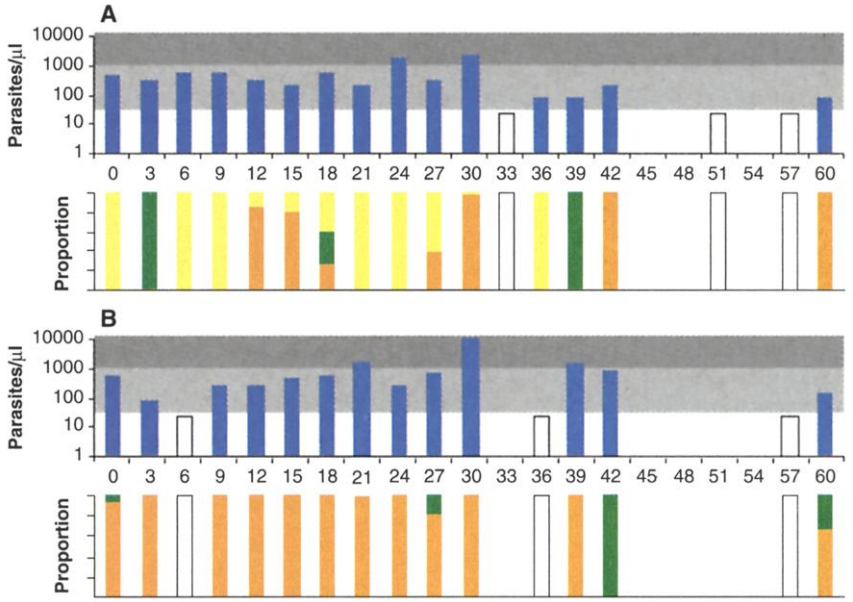

Fig. 2. Parasite dynamics in (**A**) child 19 and (**B**) child 31. Numbers between panels indicate sampling day over the 60-day period. (Upper panels) blue bars show total parasite density; light gray shading indicates the lower microscopy sensitivity level (40 parasites/μl); dark gray shading indicates the fever threshold [1000 parasites/μl (*17*)]; open bars are smear-negative samples. (Lower panels) Proportion of each species is shown for *P. falciparum* (orange), *P. vivax* (green), and *P. malariae* (yellow).

er has suggested that the species can interact. However, the relevance of such data to natural infections in individuals living in endemic regions is unclear. In such regions, individuals are superinfected from birth, whereas experimental data are derived from primary infections in nonimmune adults.

Indirect evidence for interactions between human *Plasmodium* species comes from cross-sectional malaria surveys in which there is a deficit of mixed infections relative to that expected assuming no interaction (*7*), reciprocal seasonality in the prevalence of different species (*3*, *8*), and reduction in the severity of malaria symptoms in individuals with limited pre-exposure to different species (*9*). None of these studies has provided information about parasite dynamics. To investigate the possible role of species-transcending immunity in the control of malaria parasitemia in humans, we analyzed the dynamics of multiple, coinfecting *Plasmodium* species and genotypes in infected but clinically asymptomatic children.

The intrahost dynamics of *Plasmodium* species were determined in 34 children aged 4 to 14 years, resident in Papua New Guinea (*10*). The children were exposed to all four species causing human malaria (*11*) at an estimated rate of 0.86 infectious bites per person per day (*12*). Parasites were sampled every 3 days for 60 days and species density was quantified by microscopy (*13*). Genotypes of *P. falciparum* and *P. vivax* were characterized by molecular typing (Table 1) (*14*).

Parasites were present in all 34 children (Table 1) and 82% were infected with more than one species. Many were infected with multiple *P. falciparum* and *P. vivax* genotypes (Table 1) (*14*). The number of genotypes was positively correlated with the proportion of positive smears across all age groups for *P. vivax* (Fig. 1A) ($r = 0.709$, $P = 0.002$) and in children aged 5 to 14 for *P. falciparum* (Fig. 1B) ($r = 0.742$, $P = 0.0001$). These correlations demonstrate that increased smear positivity for each species was due to more infections and not maintenance of a single genotype. Persistence of single genotypes was observed only for *P. falciparum* in children aged 4 years (Fig. 1B) (*15*).

Children with the highest proportion of smear-positive samples (Table 1) exhibited relative stability in total parasite density despite complex underlying dynamics attributable to each species (Fig. 2A). The dynamics of individual genotypes were also highly variable (*15*). The density of each species changed over time, while total parasitemia was regulated around 1000 parasites/μl of blood, for periods longer than any single episode (*16*). This value is close to fever thresholds for children in this population (*17*) and is in agreement with the absence of clinical symptoms (*10*).

We tested total parasite density data for density-dependence using Bulmer's test (*18*), which distinguishes random changes from a tendency to return to an equilibrium value. Evidence for density-dependence was detected in $\log_{10}$ total density data from all but 3 of 19 children tested (Table 1). Significance was reduced when the test was applied to each species, in 9 of 13 children with sufficient data to test, indicating the cross-species nature of regulation. Where a single species predominated but multiple genotypes were present (children number 6, 31, 4, 32, and 14), total parasitemia also exhibited density-dependence (Fig. 2B and Table 1), suggesting that single-species coinfections are regulated similarly. Maintenance of total parasite density around a threshold is inconsistent with dynamics resulting only from species- and/or genotype-specific immunity responsible for parasite clearance [reviewed in (*19*)]. To account for these dynamics, additional species-transcending, density-dependent regulation of parasite density is required.

To determine if there was evidence for interactions between species, we analyzed the patterns of infection in the children. The number of children infected with >1 species during

[1]Wellcome Trust Centre for the Epidemiology of Infectious Disease, Department of Zoology, University of Oxford, Oxford, OX1 3FY, UK. [2]Papua New Guinea Institute of Medical Research, Post Office Box 378, Madang, Papua New Guinea. [3]Department of Medicine, Division of Infectious Diseases, Emory University School of Medicine, Emory Vaccine Center at Yerkes, Atlanta, GA 30329, USA. [4]Biology and Diagnostic Branch, Division of Parasitic Diseases, Centers for Disease Control and Prevention, Atlanta, GA 30341, USA. [5]Institute of Cell, Animal and Population Biology, University of Edinburgh, Edinburgh, EH9 3JN, UK.

*To whom correspondence should be addressed. E-mail: marian.bruce@ceid.ox.ac.uk

Table 1. Microscopy, genotyping, and statistical results. The Bulmer test (*18*) was not used on data from 13 children with <50% positive smears and two children with autocorrelated total parasite density data (*24*). "nd" indicates not done. Dashes indicate where a species was not detected. *Pf*, *P. falciparum*; *Pv*, *P. vivax*; *Pm*, *P. malariae*; *Po*, *P. ovale*.

ID	Age	Sex	Blood smears	Proportion of smears positive (any species)	Positive smears				Species detected*	Genotypes		Episodes§			Bulmer test on density (*P*)			
					Pf	*Pv*	*Pm*	*Po*		*Pf*†	*Pv*‡	*Pf*	*Pv*	*Pm*	Total	*Pf*	*Pv*	*Pm*
5	4	m	16	1.00	14	10	0	0	2	2	7	2	4	0	0.05	0.01	>0.05	–
1	4	m	16	0.94	7	10	0	0	2	1	4	3	2	0	0.0005	nd	>0.05	–
12	8	m	19	0.84	11	5	7	0	3	5	1	3	3	3	0.025	0.025	nd	nd
19	14	m	18	0.83	7	3	11	0	3	5	nd	4	3	3	0.025	nd	nd	>0.05
6	7	m	11	0.82	8	1	1	0	3	6	nd	2	1	1	0.025	0.025	nd	nd
31	10	m	16	0.81	12	4	0	0	2	9	4	3	4	0	0.0005	0.005	nd	–
33	10	f	15	0.80	5	10	0	0	2	3	7	3	4	0	nd			
34	14	m	15	0.80	10	3	1	0	3	5	nd	3	2	1	0.0005	0.01	nd	nd
25	12	m	14	0.79	5	2	6	0	3	5	nd	2	2	4	>0.05	nd	nd	nd
4	4	f	12	0.75	7	2	0	0	2	1	1	1	1	0	0.005	>0.05	nd	–
24	14	m	16	0.75	3	8	2	0	3	1	8	3	3	2	0.05	nd	>0.05	nd
22	14	f	19	0.74	10	4	1	0	3	4	3	4	4	1	0.0005	0.005	nd	nd
32	13	m	19	0.74	12	3	0	0	2	5	nd	2	3	0	0.0005	0.0005	nd	–
16	7	f	15	0.73	8	8	1	1	4	6	6	2	2	1	nd			
20	14	m	16	0.69	6	6	1	0	3	6	3	1	6	1	0.0005	nd	nd	nd
14	6	f	19	0.63	0	11	1	0	2	nd	3	0	5	1	0.005	–	0.025	nd
18	5	f	15	0.60	5	5	0	0	2	4	3	4	2	0	0.05	nd	nd	–
29	11	f	12	0.58	1	2	5	0	3	nd	nd	1	2	2	>0.05	nd	nd	nd
17	6	m	18	0.56	7	2	1	0	3	4	nd	2	1	1	0.001	nd	nd	nd
2	4	m	18	0.50	9	0	0	0	1	1	nd	4	0	0	0.001	0.001	–	–
26	12	m	18	0.50	4	2	3	0	3	4	nd	2	2	2	>0.05	nd	nd	nd
11	9	f	13	0.46	4	2	0	0	2	5	nd	2	2	0	nd			
10	8	m	16	0.44	3	5	0	0	2	5	3	2	4	0	nd			
15	9	f	19	0.42	1	6	1	0	3	nd	4	1	6	1	nd			
7	7	m	18	0.39	5	1	1	0	3	3	nd	3	1	1	nd			
8	7	f	19	0.37	2	5	0	0	2	3	1	2	3	0	nd			
28	11	f	18	0.33	2	0	4	0	2	1	nd	1	0	1	nd			
27	10	f	19	0.32	1	5	0	0	2	nd	4	1	3	0	nd			
21	11	f	18	0.22	4	0	0	0	1	2	nd	2	0	0	nd			
9	7	m	16	0.19	1	2	0	0	2	nd	nd	1	1	0	nd			
23	11	f	16	0.19	0	3	0	0	1	nd	nd	0	2	0	nd			
13	5	f	17	0.12	0	2	0	0	1	nd	nd	0	2	0	nd			
30	11	f	19	0.11	0	2	0	0	1	nd	nd	0	2	0	nd			
3	4	m	13	0.08	0	1	0	0	1	nd	nd	0	1	0	nd			

*By microscopy (*13*). †Determined by analysis of *PfMsp2* alleles (*14*). ‡Determined by analysis of *PvMsp3α* alleles (*14*). §Determined from microscopy data (*16*).

the study was no different from that expected, assuming independence of each species (χ^2 = 1.60, 2 df, P = 0.449). In contrast, a deficit of mixtures of species was detected when data were analyzed cross-sectionally (χ^2 = 9.06, 2 df, P = 0.028). The peak density of episodes of different species (*16*) did not coincide as often as expected by chance (χ^2 = 6.56, 1 df, P = 0.010). Together, these results demonstrate that episodes tended to follow a sequential rather than a concurrent pattern.

Sequential infections with different *Plasmodium* species have been reported from a few other longitudinal data sets [reviewed in (*1*)], but these were not interpreted as the effect of density-dependent regulation. In symptomatic, nonimmune individuals, fever may underlie the stability of parasitemia (*20*), but in these single infections the *Plasmodium* immune evasion mechanism of antigenic variation (*19*) could also explain these dynamics (*21*). Fever prevalence in children aged 4 to 14 in Papua New Guinea is insufficient to fully account for our data (*17*). Neither antigenic variation nor density-dependent regulation alone can explain both the stability of parasitemia and sequential infections observed in our data.

We believe that the species interactions result from the interplay between density-dependent regulation and the differential growth and clearance rates of individual parasite populations resulting from clonal antigenic variation (*19*, *22*). Growth of one parasite population to above threshold density will trigger density-dependent regulation. When this happens, minority coinfections will also be inhibited. When the majority population is cleared by species- and/or genotype-specific responses (*19*, *22*), total density will drop below the threshold and density-dependent regulation will cease. In these circumstances, minority populations could expand because density-dependent constraints would be absent. In this way, the sequential episodes of infection we have observed can be generated.

If species-specific vaccines [e.g., (*23*)] are successful in reducing or preventing *P. falciparum* parasitemia, the effect in highly endemic regions could be to provide an increased opportunity for other species to multiply when the constraint imposed by density-dependent regulation is removed. This could result in increased prevalence, transmission potential, and disease unless vaccines include targets specific for other species.

References and Notes

1. T. L. Ritchie, *Parasitology* **96**, 607 (1988).
2. H. A. Babiker, A. M. Creasey, R. A. L. Bayoumi, D. Walliker, *Trans. R. Soc. Trop. Med. Hyg.* **85**, 578 (1991); R. E. L. Paul *et al.*, *Science* **269**, 1709 (1995); F. Ntoumi *et al.*, *Am. J. Trop. Med. Hyg.* **52**, 81 (1995).
3. K. Maitland, T. N. Williams, C. I. Newbold, *Parasitol. Today* **13**, 227 (1997).
4. M. Ciuca, L. Ballif, M. Chelarescu-Vieru, *Trans. R. Soc. Trop. Med. Hyg.* **27**, 619 (1934); W. H. Taliaferro, in *Malariology*, M. F. Boyd, Ed. (Saunders, Philadelphia, 1939); G. M. Jeffery, *Bull. WHO* **35**, 873 (1966).
5. M. F. Boyd and S. F. Kitchen, *Am. J. Trop. Med.* **17**, 855 (1937); *Am. J. Trop. Med.* **18**, 505 (1938).
6. M. F. Boyd, W. H. Kupper, C. B. Matthews, *Am. J. Trop. Med.* **18**, 521 (1938).
7. J. E. Cohen, *Q. Rev. Biol.* **48**, 467 (1973); K. Maitland *et al.*, *Trans. R. Soc. Trop. Med. Hyg.* **90**, 614 (1996).
8. L. Molineaux, J. Storey, J. E. Cohen, A. Thomas, *Am. J. Trop. Med. Hyg.* **29**, 725 (1980).
9. D. M. Gunewardena, R. Carter, K. N. Mendis, *Mem. Inst. Oswaldo Cruz Rio J.* **89**, 61 (1994); N. D. Ka-

runaweera, R. Carter, G. Grau, K. N. Mendis, *Am. J. Trop. Med. Hyg.* **58**, 204 (1998).
10. This study was carried out in the village of Gonoa, Madang Province, Papua New Guinea, between 28 June and 27 August 1992 (*15*). Children ≥4 years old were enrolled following informed consent from parents or guardians. Clinical malaria and drug use was monitored by self-reporting. One child reporting fever was eliminated from the study. Only children with ≥50% compliance with sampling were used in analyses. Ethical clearance was granted by the Medical Research Advisory Committee of Papua New Guinea, who recommend that asymptomatic malaria infections should not be treated in order to allow natural, protective immunity to develop.
11. J. A. Cattani *et al.*, *Am. J. Trop. Med. Hyg.* **35**, 3 (1986).
12. Combined mean number of infectious bites per person per day for the two most prevalent species, *P. falciparum* and *P. vivax* [T. R. Burkot, P. M. Graves, J. A. Cattani, R. A. Wirtz, F. D. Gibson, *Bull. WHO* **65**, 375 (1987)].
13. Parasite species density was obtained from thick and thin blood smears. Smears were air-dried, thin smears were fixed in methanol, and both were stained in 4% Giemsa in sodium phosphate buffer (pH 7.2) for 45 min. Enumeration was per 200 leukocytes and counts were converted to parasites/μl of blood, assuming 8000 leukocytes/μl.
14. All samples were analyzed from children with ≥2 *P. falciparum* smear-positive samples or ≥4 *P. vivax* positives (*15*). Blood from finger pricks was collected in EDTA and stored at −70°C, then 20-μl volumes were transferred to filter paper for DNA extraction [S. Kyes, A. G. Craig, K. Marsh, C. I. Newbold, *Exp. Parasitol.* **77**, 473 (1993)]. *Plasmodium falciparum* genotypes were determined by size and sequence polymorphisms in PCR-amplified alleles of the *merozoite surface protein 2* (*Msp2*) gene [H. Babiker, L. Ranford-Cartwright, A. Sultan, G. Satti, D. Walliker, *Trans. R. Soc. Trop. Med. Hyg.* **88**, 328 (1994)]. *Plasmodium vivax* genotypes were determined by polymerase chain reaction–restriction fragment length polymorphism (PCR-RFLP) analysis [M. C. Bruce, M. R. Galinski, J. W. Barnwell, G. Snouou, K. P. Day, *Am. J. Trop. Med. Hyg.* **61**, 518 (1999)] of alleles at the *merozoite surface protein 3 alpha* (*Msp3α*) locus [M. R. Galinski *et al.*, *Mol. Biochem. Parasitol.* **101**, 131 (1999)].
15. M. C. Bruce *et al.*, *Parasitology*, in press.
16. Episodes were quantified by consecutive smear-positive time points for *P. vivax* and *P. malariae*. Consecutive or 6-day positive time points were used for *P. falciparum* to adjust for periodicity resulting from synchronous growth and sequestration [(*15*); A. Färnert, G. Snounou, I. Rooth, A. Björkman, *Am. J. Trop. Med. Hyg.* **56**, 538 (1997)].
17. M. J. Cox *et al.*, *Trans. R. Soc. Trop. Med. Hyg.* **88**, 191 (1994).
18. M. G. Bulmer, *Biometrics* **31**, 901 (1975); D. R. Fox and J. Ridsdill-Smith, *Oecologia* **103**, 435 (1995). Zero microscopy values were replaced with 1 in autocorrelation and Bulmer tests.
19. K. N. Brown, *Immunol. Lett.* **25**, 97 (1990).
20. D. Kwiatkowski, *Parasitol. Today* **11**, 206 (1995).
21. T. Staalsoe and L. Hviid, *Parasitol. Today* **14**, 177 (1998).
22. K. N. Brown and I. N. Brown, *Nature* **208**, 1286 (1965).
23. C. F. Ockenhouse *et al.*, *J. Infect. Dis.* **177**, 1664 (1998).
24. H. Wolda and B. Dennis, *Oecologia* **95**, 581 (1993).
25. We thank the people of Gonoa for their long-standing cooperation and the staff of the Papua New Guinea Institute of Medical Research, Madang, for their assistance. Supported by grants to K.P.D., D.W., and M.P.A. from the European Commission, by a grant to K.P.D. from the Wellcome Trust, by NIH grant AI24710 to J.W.B., and NIH grant AI37545 and World Health Organization/TDR grants (950440 and 910495) to M.R.G. M.C.B. was supported by The UK Medical Research Council and The Wellcome Trust. C.A.D. was supported by The Wellcome Trust.

27 July 1999; accepted 15 December 1999

Mutations in *SDHD*, a Mitochondrial Complex II Gene, in Hereditary Paraganglioma

Bora E. Baysal,[1]* Robert E. Ferrell,[2] Joan E. Willett-Brozick,[1] Elizabeth C. Lawrence,[2] David Myssiorek,[5] Anne Bosch,[6] Andel van der Mey,[7] Peter E. M. Taschner,[6] Wendy S. Rubinstein,[3] Eugene N. Myers,[4] Charles W. Richard III,[9] Cees J. Cornelisse,[8] Peter Devilee,[6] B. Devlin[1]

Hereditary paraganglioma (PGL) is characterized by the development of benign, vascularized tumors in the head and neck. The most common tumor site is the carotid body (CB), a chemoreceptive organ that senses oxygen levels in the blood. Analysis of families carrying the *PGL1* gene, described here, revealed germ line mutations in the *SDHD* gene on chromosome 11q23. *SDHD* encodes a mitochondrial respiratory chain protein—the small subunit of cytochrome b in succinate-ubiquinone oxidoreductase (cybS). In contrast to expectations based on the inheritance pattern of PGL, the SDHD gene showed no evidence of imprinting. These findings indicate that mitochondria play an important role in the pathogenesis of certain tumors and that cybS plays a role in normal CB physiology.

Regulation of oxygen homeostasis is essential for most organisms (*1*). In mammals, the CB, a highly vascular small organ located at the bifurcation of the common carotid artery in the neck, plays a major role in acute adaptation to hypoxia (oxygen deprivation) by stimulating the cardiopulmonary system (*2*). At the cellular level, this adaptation involves activation of a transcription factor, hypoxia-inducible factor–1 (HIF-1), which subsequently leads to a systemic response, including an increase in red blood cell mass, stimulation of new blood vessel growth, and increased ventilation (*3*). Chronic exposure to hypoxia (e.g., as occurs in individuals dwelling at high altitudes or in those with certain medical conditions, such as cyanotic heart and chronic lung diseases) induces cellular hyperplasia/anaplasia in the CB (*4*).

The CB is also the most common tumor site for hereditary paraganglioma (PGL), a rare disorder characterized by the development of mostly benign, highly vascular, slow-growing tumors in the head and neck. PGL tumors display cellular hyperplasia/anaplasia (*5*) in the absence of any hypoxic stimulus. A gene responsible for PGL was mapped to chromosome band 11q23 (*PGL1*) and remains the only locus confirmed in independent families (*6–8*). *PGL1* is inherited in an autosomal dominant fashion with incomplete penetrance when transmitted through fathers, whereas no disease phenotype occurs when transmitted maternally. This inheritance pattern is observed in all confirmed *PGL1* pedigrees and suggests that there is sex-specific epigenetic modification of *PGL1* during gametogenesis, consistent with genomic imprinting (*9*). This consistent inheritance pattern gives PGL a unique place among the known human genetic disorders with parent-of-origin effects (*10*). Several features of PGL tumors, including their benign biological behavior, limited organ involvement, and histopathology, are markedly similar to those of chronic hypoxia-stimulated CBs. This led us to hypothesize that the genetic defect in *PGL1* involves a critical component in the oxygen-sensing and -signaling pathway.

We previously localized *PGL1* to an approximately 1.5-Mb critical interval between D11S1986 and D11S1347 (*8*). BAC and yeast artificial chromosome (YAC) contig construction and discovery of 16 new simple tandem repeat polymorphisms (STRPs) (*11*) enabled us to confine *PGL1* to an approximate 400-kb region (*12*) flanked by the recombination breakpoints in families 5 (*7*) and 12 (*8*) (Fig. 1).

Expressed sequence tag (EST) gene content mapping of transcripts (*13*) revealed a high density of transcripts in the 400-kb *PGL1* critical region and in its close vicinity (*11*). A database search using BLAST with one of the ESTs in the critical region,

[1]Department of Psychiatry, [2]Department of Human Genetics, [3]Pittsburgh Cancer Institute, [4]Department of Otolaryngology, The University of Pittsburgh Medical Center, Pittsburgh, PA 15213–2593, USA. [5]Department of Otolaryngology and Communicative Disorders, Long Island Jewish Medical Center, New Hyde Park, New York, NY 11040, USA. [6]Department of Human Genetics, [7]Department of Otolaryngology, [8]Department of Pathology, Leiden University Medical Center, 2300 RA, Leiden, Netherlands. [9]Wyeth-Ayerst Research, Genetics Institute, 35 Cambridgepark Drive, Cambridge, MA 02140, USA.

*To whom correspondence should be addressed. E-mail: baysalbe@msx.upmc.edu